



Validation and analysis of detailed kinetic models for ethylene combustion

Chaoqi Xu^{a,b}, Alexander A. Konnov^{a,*}

^a Division of Combustion Physics, Department of Physics, Lund University, P.O. Box 118, SE-221 00 Lund, Sweden

^b National Key Laboratory of Combustion, Flow and Thermo-Structure, Northwestern Polytechnical University, 710072 Xi'an, People's Republic of China

ARTICLE INFO

Article history:

Received 19 June 2011

Received in revised form

29 September 2011

Accepted 4 November 2011

Available online 2 December 2011

Keywords:

Ethylene

Ignition

Flame propagation

Model validation

ABSTRACT

Present work aims at evaluation of contemporary comprehensive detailed kinetic mechanisms for ethylene combustion, including the Konnov mechanism, LLNL nButane mechanism, San Diego (UCSD) mechanism and USC mechanism. These models have been validated by extensive comparison with available experimental data on ethylene ignition and flame propagation. The experimental data from the literature have been carefully examined to accurately assess the models' predicting performance. Noticeable differences in the predictions of ethylene ignition and flame propagation under a variety of conditions have been observed. Moreover, sensitivity analysis has been conducted to identify important reactions for the prediction of ethylene ignition and flames. For ethylene ignition, it was found that C₂H₄ consumption reactions with radicals OH, O and subsequent reactions of vinyl with oxygen have dominant effect on predicted ignition delays. The pathway analysis has also been performed for each mechanism to identify different reaction pathways in ethylene ignition process. For ethylene flames, sensitivity analysis shows that H–O and C₁ chemistry reactions significantly influence the laminar burning velocity in lean ethylene/air flames, while C₂ chemistry reactions become of increasing importance in fuel-rich flames. Furthermore, to better understand the models' predicting behavior, the differences in the reaction rate constants and routes of C₂H₄ and vinyl chemistry have been analyzed and discussed.

© 2011 Elsevier Ltd. All rights reserved.

1. Introduction

Ethylene has received a wide research interest in recent years, since it is a key intermediate in the oxidation of higher alkanes and alkenes, and thereby plays an important role in the combustion chemistry of most practical fuels. It is one of the most important petrochemicals produced through steam cracking [1]. Moreover, ethylene itself is a very reactive fuel as well as a typical cracking and decomposition product of storable JP-type hydrocarbon fuels for high-speed airbreathing propulsion applications, such as pulse detonation engines and Scramjet [2]. Recent advances in the development of detailed chemical kinetic mechanisms for hydrocarbon fuels considerably help not only in deep understanding of combustion phenomena, but also in accurately predicting combustion processes, such as ignition, flame propagation and extinction characteristics which are the key parameters for combustion applications.

Ignition delay time and laminar flame burning velocity are crucial characteristics of fuel combustion from both fundamental and practical considerations and often used as key parameters for chemical kinetic mechanisms validation and optimization. A considerable amount of available experimental data on ethylene ignition and flames has been reported over the past several decades. Several detailed kinetic mechanisms [3–6] for ethylene combustion have been proposed and developed to reproduce, *inter alia*, available experimental data on ethylene oxidation. However, due to remaining uncertainties both in the rates and reaction pathways among different detailed kinetic mechanisms, noticeable discrepancies in the prediction behaviors of ethylene ignition and flames have been observed.

The purpose of the present study was validation and analysis of several contemporary comprehensive detailed kinetic mechanisms for ethylene combustion, including the Konnov mechanism [3], LLNL nButane mechanism [4], San Diego mechanism [5] and USC mechanism [6]. One should note that although the model from LLNL was validated for n-Butane [7] (hence the name) it was also validated for flames of methane, ethane, ethylene and propane [4]. In order to precisely assess modeling results, experimental data for ethylene ignition and flames from the literatures have been

* Corresponding author. Tel.: +46 462229757; fax: +46 462224542.

E-mail address: Alexander.Konnov@forbrf.lth.se (A.A. Konnov).

Table 1
Summary of available C₂H₄/O₂ ignition delay experiments in shock tubes.

| Equivalence ratio ϕ | % Diluent (Ar) | P(atm) | T(K) | Ignition criteria/Detection method | Ref. |
|--------------------------|------------------------------------------|-----------|-----------|------------------------------------------------------------------|------|
| 0.21–3.5 | 96–99 | 0.2–0.4 | 1450–2350 | CH* onset/Incident shock | [10] |
| 0.5, 1.5 | 98.5, 96.5 | 0.3–0.8 | 1500–2300 | CO + CO ₂ emission 10% of max | [11] |
| 1, 1.5, 2 | 84, 85, 92–95 | 1.0–2.2 | 1090–1650 | OH* max | [12] |
| 0.125–2 | 93–99 | 3, 12 | 1000–1900 | OH* max/Sidewall | [13] |
| 0.46–2.63 | 70 | 1–3.2 | 800–1400 | OH* absorption max rate of change | [14] |
| 0.5, 1, 1.5 | 91–93 | 1.1–1.7 | 1815–2365 | CO + CO ₂ emission for [O][CO] maximum/Incident shock | [15] |
| 1, 1.5, 3 | 98, 97, 96 | 1–5 | 1400–2100 | CH* onset/Sidewall | [16] |
| 0.5, 1, 2 | 96.5–99.3 | 1.5–4.5 | 1100–2100 | CO ₂ emission onset | [17] |
| 1 | 96, 75 | 1–3 | 1000–1800 | CH* onset/Endwall | [18] |
| 1, 1.5 | 50(N ₂), 75(N ₂) | 1–4 | 800–1620 | CH* onset/Sidewall | [19] |
| 0.5, 0.75, 1 | 95–97 | 3–8 | 1100–1500 | OH* onset/Sidewall | [2] |
| 1 | 84, 92, 96 | 1.1–4 | 1253–1572 | CH* max/Sidewall | [20] |
| 0.5, 1 | 96, 98 | 0.9–3.3 | 1115–1900 | OH* onset, OH* max/Endwall | [21] |
| 0.5, 1, 2 | 77.5, 75, 70.5(N ₂) | 5.9–16.5 | 1060–1520 | CH* onset, C ₂ onset, OH onset/Endwall | [22] |
| 1, 3 | 93, 96, 98 | 2, 10, 18 | 1000–1650 | CH* onset, OH* onset, Visible light/Endwall | [23] |

carefully examined and then were used to compare with the modeling. Also, sensitivity and reaction pathways analyses at different conditions were employed for analysing the predicting behavior of the models.

2. Ignition delays

2.1. Available experimental data

Many ignition experiments have been conducted to build and extend ignition delay time database and also to compare with previous studies and model predictions. Numerous researchers [8–23] investigated ignition of ethylene highly diluted by argon or nitrogen in shock tubes which can provide the near-constant-volume reaction conditions with well-defined temperatures and pressures [24]. Available experimental data for ethylene ignition are summarized in Table 1. Most ethylene shock tube studies prior to 1999 were summarized in the work of Schultz and Shepherd [8]. In the recent studies, Horning [20] performed ethylene ignition ($\phi = 1$) experiments at pressures 1–4 atm, covering a temperature range of ~1250–1700 K by monitoring CH* emission maximum. The effects of pressure and diluent argon on ignition delay time were studied, and it was found that the ignition delay times were longer at higher dilutions and lower pressures. Saxena et al. [23] conducted experiments with different dilutions (Ar = 93%, 96%, 98%) in reflected shock waves over a temperature range of 1000–1650 K at pressures of 2, 10 and 18 atm, equivalence ratio of 3 and 1. In their study, the ignition delay times showed little variation with pressure and equivalence ratio at the conditions of 93% argon dilution, while the longer ignition delay times were observed at lower pressures for higher diluted mixtures (Ar = 96%, 98%). The authors also compared their experimental results with the predictions of the optimized version of USC mechanism and found that the model shows a very good agreement at high pressures ($P = 10$ and 18 atm), but over-predicts the ignition delay times in low temperature range (less than 1250 K) at low pressures. Varatharajan and Williams [9] summarized the previous experimental ethylene ignition delay results, and validated their detailed ethylene reaction mechanism by using these experimental data. They concluded that their modeling results indicated good agreement with the high-temperature data (above 1500 K), e.g. [17], whereas at lower temperatures, the ignition times were very sensitive to the choice of the ignition criterion.

Numerous ethylene ignition data have been obtained under a variety of experimental conditions, however, it is difficult to compare these data directly due to the differences in the ignition detection method and ignition definition in these studies. When

performing detailed kinetic model validation, it is necessary to carefully consider the discrepancies among different ignition delay time studies. Horning [20] noted that the ignition times recorded at the shock tube sidewall may be significantly shorter than those measured at the endwall due to perturbations caused by potential non-ideal gas-dynamic effects resulted from the energy release of the reaction, especially for highly energetic mixtures at higher temperatures. Kalitan et al. [21] presented comparison of ignition delay times obtained from endwall and sidewall emission traces. The results showed the sidewall ignition was accelerated slightly at the higher temperatures and could be as much as 30% faster than the endwall results at about 1700 K and 1 atm for stoichiometric mixture with 98% argon dilution. Additional effects need to be considered include the actual definition of ignition delay time. Usually ignition criteria is based on maximum or onset emission of combustion intermediate species such as CH* or OH*. Varatharajan and Williams [9] have confirmed that the ignition times predicted by different criteria can typically differ by a factor of about two at high temperature and low pressure. These experimental details can be quite important, particularly when comparing measurements with the results of modeling or other experiments that might be based on different diagnostics methods and definitions of ignition.

To facilitate direct comparison of experimental data under different conditions, correlations of ignition delay time with composition and temperature were usually utilized. The most popular correlation form is as following:

$$\tau = Z[C_2H_4]^a [O_2]^b [Ar]^c e^{-E_a/RT} \quad (1)$$

where Z is scaling constant, $[i]$ is the concentration of reactant i , T is mixture temperature and E_a is the overall activation energy. Remarkably, a number of largely different correlations have been proposed. Most studies identified strong dependence of ignition delay on oxygen concentration (power exponent b in Eq. (1) varies from -1.2 to -0.83), and weak dependence of ignition on ethylene concentration (power exponent a varies from 0 to 0.3). Colket and Spadaccini [2] and Kalitan et al. [21] believed the argon concentration dependency is negligible, while Saxena et al. [23] considered the argon concentration dependency reasonably significant. In addition, activation energy variations from 17.1 to 35 kcal/mol were found in previous studies. This might be due to the different ranges of temperature, composition and pressure. Horning [20] has found the ignition time of ethylene showed increasing overall activation energy with increasing pressure in the range of 1–4 atm.

Since ethylene ignition delay data were obtained over a wide range of experiment conditions and with different definitions of

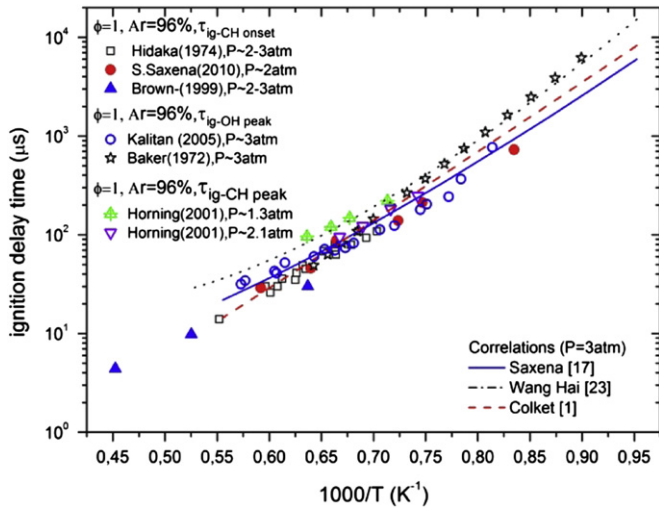


Fig. 1. Comparison of ethylene ignition delay data at $\phi = 1$, $Ar = 96\%$ ($P \sim 1\text{--}3$ atm) and correlations for ignition delays at $P = 3$ atm.

ignition, the apparent discrepancies were found. Therefore, in order to focus the analysis of the ignition delay data and model evaluation, only the comparison of the stoichiometric ethylene ignition delays and some correlations [2,23,25] at similar conditions (low pressure, $Ar = 96\%$ and 92%) are respectively presented in Figs. 1 and 2.

For $\phi = 1$, $Ar = 96\%$ conditions, the comparison shows obvious disagreement between experimental data of Baker and Skinner [13] and of Kalitan et al. [21] based on OH^* maximum emission criteria at pressures about 3 atm. The ignition delay times of Baker and Skinner [13] possess stronger temperature dependency that leads to longer delay times at low temperatures and shorter delay times at higher temperatures as compared to the data of Kalitan et al. [21] and correlations obtained by Saxena et al. [23] and Colket and Spadaccini [2]. Measurements of Hidaka et al. [16] and of Brown and Thomas [18] are in good consistency with those of Baker and Skinner [13] at high temperatures, however their data were obtained based on CH^* emission onset which should give shorter delays than the results obtained based on OH^* emission maximum as will be shown in the following. Many researchers have indicated that ignition delay time is sensitive to pressure at low pressures and is shorter for higher pressures. The delay times obtained by Saxena et al. [23], and by Horning [20] at pressures about 2 atm are similar

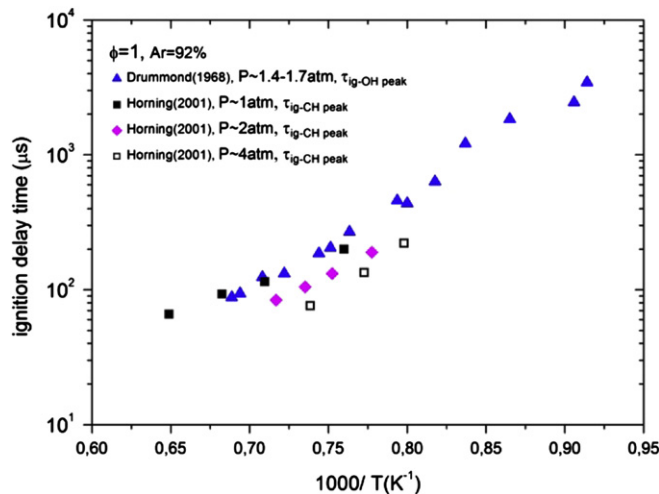


Fig. 2. Comparison of ethylene ignition delay data at $\phi = 1$, $Ar = 92\%$ ($P \sim 1\text{--}4$ atm).

to those of Baker and Skinner [13] and Kalitan et al. [21] at pressures about 3 atm, which can be due to the ignition delay time based on CH onset and CH maximum are to be shorter than the data based on OH maximum, as shown in Fig. 3 and discussed in the following.

For $\phi = 1$, $Ar = 92\%$ conditions, measurements of Horning [20] show the effect of pressure on ignition delay. As shown in Fig. 2, the agreement between the ignition delay times obtained by Drummond [12] using OH maximum criteria at pressures about 1.4–1.6 atm and Horning [20] using CH maximum criteria at pressure about 1 atm is reasonable.

2.2. Modeling details

Chemkin-Pro closed homogeneous batch reactor model [26] with constant-volume adiabatic assumption was used for the simulations of ethylene ignition process. Fig. 3(a) shows typical predicted temperature, CH and OH concentration profiles as a function of time at $\phi = 1$, $Ar = 96\%$ $P \sim 2$ atm. As can be seen, OH concentration typically shows fast increasing after a low concentration and slow “preignition” process, and then relatively slow decline occurs during a period of time. That may lead to uncertainty and difficulty to determine ignition delay time when using OH maximum as ignition criteria for model validation. In contrast, CH experiences a rapid increase and drop over very short time. CH maximum can be readily defined, and it was found that CH

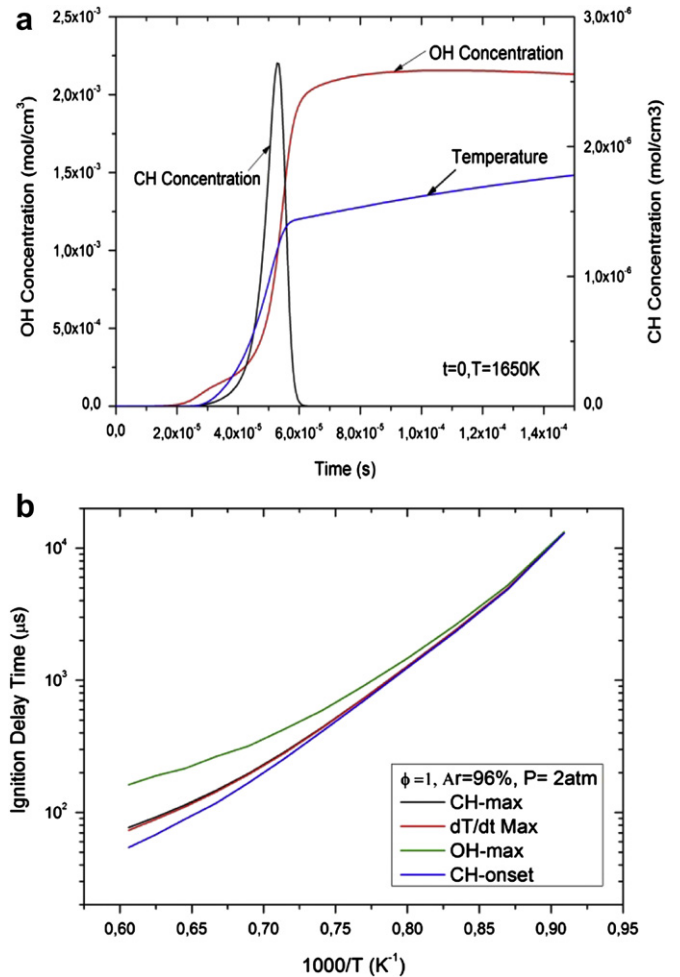


Fig. 3. Typical model predictions (the Konnov model [3]): (a). OH , CH concentrations and temperature profile (b). predicted ignition delay times defined using different criteria.

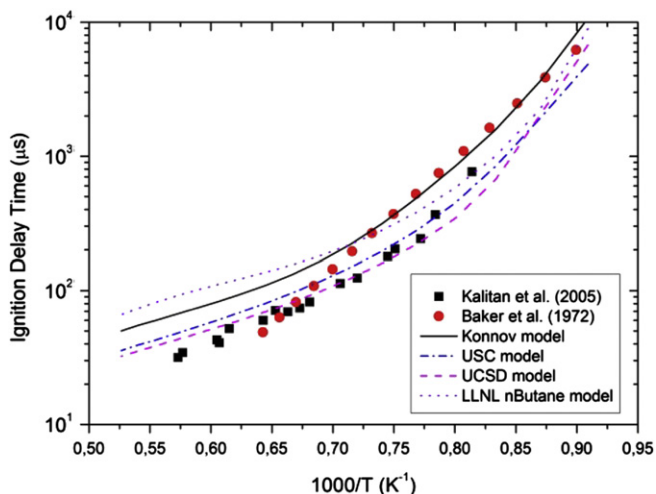


Fig. 4. Comparison of experimental ignition delay times (symbols) with prediction results (lines) using different models at $\phi = 1$, Ar = 96%, $P \sim 3$ atm.

maximum ignition time was much closer to the maximum temperature change. In addition, the species onset ignition time is also difficult to be well defined due to instrumental dependency. Therefore, it is better and convenient to use CH maximum as experimental ignition definition for model validation. As shown in Fig. 3(b), predicted ignition delay times using different ignition criteria could differ significantly at high temperatures.

Most of experimental ignition delays are based on the concentrations of electronically excited CH^* and OH^* . These excited species are not necessarily in a straightforward relationship with ground-state radicals CH and OH. A fair comparison of the experiments and modeling therefore should include prediction of these excited species. Wangher et al. [27] compared model predictions of OH^*

combining chemiluminescence sub-mechanisms of Hall et al. [28] and of Haber and Vandsburger [29] with the GRI-mech. and with the Konnov reaction mechanisms. They found significant discrepancies between these two models and concluded that further development of the chemiluminescence sub-mechanisms is required. None of the mechanisms analyzed in the present work include excited species; hence, to avoid additional ambiguity, they were not supplemented by still uncertain chemiluminescence sub-mechanisms. On the other hand, Hall et al. [28] concluded that CH^* follows CH peak within 5% over most of the conditions studied, while OH and OH^* ignition times were found to be consistent only for $T < 1600$ K. For $T > 1600$ K, OH and OH^* ignition error may be as great as 30%. This should be kept in mind when comparing experiments and model predictions discussed below.

2.3. Comparison of the experiments and models

In the following the calculations based on OH maximum and CH maximum were performed for model evaluation to respectively compare with the experimental data of Baker and Skinner [13] and Kalitan et al. [21] at $\phi = 1$, Ar = 96% conditions and those of Horning [20] at $\phi = 1$, Ar = 92%. Comparisons of the stoichiometric ethylene ignition delay times at Ar = 96%, $P \sim 3$ atm conditions are presented in Fig. 4.

The calculations using the Konnov mechanism are in very good agreement with the experimental data from Baker and Skinner [13] in low temperature range ($1100 < T < 1400$ K), and overpredict the experimental data as temperature is increasing. Additionally, the Konnov mechanism overpredicts the experimental data obtained by Kalitan et al. [21] throughout their experimental temperature range, typically by a factor of two. While the modeling using UCSD and USC mechanisms gives very good agreement with Kalitan et al. [21] results, they underpredict the data of Baker and Skinner [13] in lower temperature range. LLNL nButane model cannot reproduce

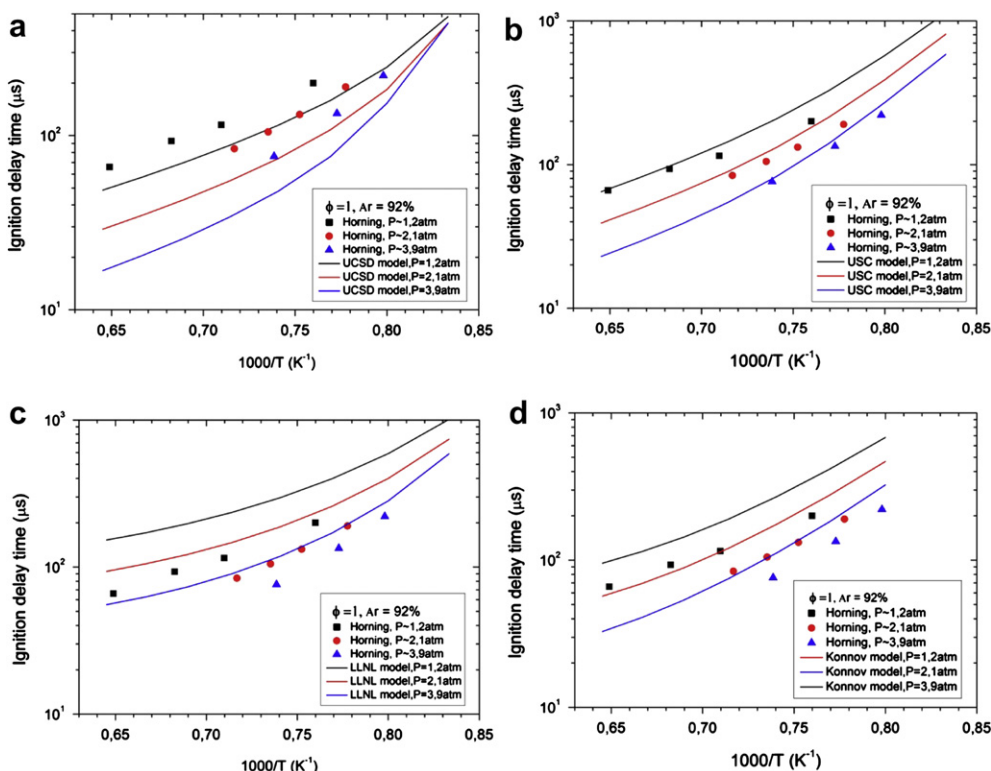


Fig. 5. Comparison of experimental data at $\phi = 1$, Ar = 92% [20] (symbols) and prediction results (lines) using different models.

well these experiment data, the prediction results are in between the Konnov and USC models at low temperature ($T < 1400$ K), and overprediction becomes more severe with increasing temperature.

Fig. 5 presents comparison of experimental data obtained by Horning [20] and predicted ignition delays using different mechanisms for 92% argon diluted stoichiometric C_2H_4/O_2 mixture at different pressures. As can be seen, the modeling results using USC mechanism show the best agreement with the experimental data over entire temperature range at different pressures, especially for high temperature region. The Konnov modeling results overpredict the experiment data typically by about a factor of 2 at these conditions, while the UCSD mechanism underpredicts the experimental ignition delays within a factor of 2. LLNL nButane mechanism obviously overpredicts the experiment data, especially at low pressure conditions. Besides, in all cases, only UCSD mechanism predicts notable overall activation energy change with the pressure which was experimentally observed by Horning [20].

2.4. Modeling analysis

Brute-force sensitivity analysis was performed to identify important reactions in the ethylene ignition process. The sensitivities of ignition delay time based on CH maximum criteria for stoichiometric mixture (Ar = 92%) at pressure 2.1 atm and temperature 1350 K are presented in Fig. 6. Sensitivity analysis shows that C_2H_4 initial consumption reactions with radicals O and

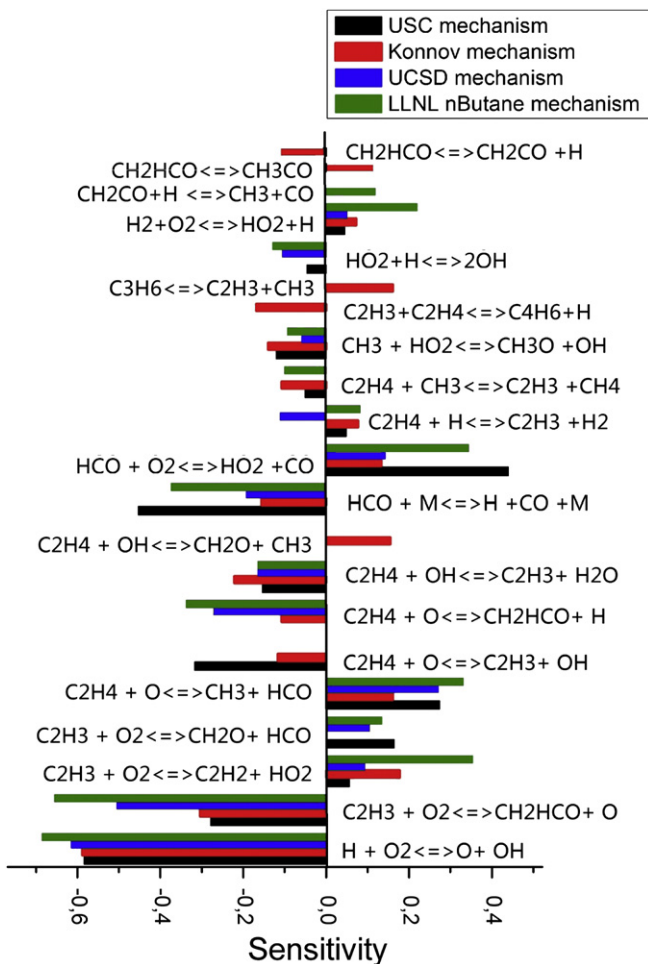


Fig. 6. Sensitivities of ignition delay time based on CH maximum criteria using different mechanisms for $\theta = 1$, Ar = 92%, $P = 2.1$ atm and $T = 1350$ K.

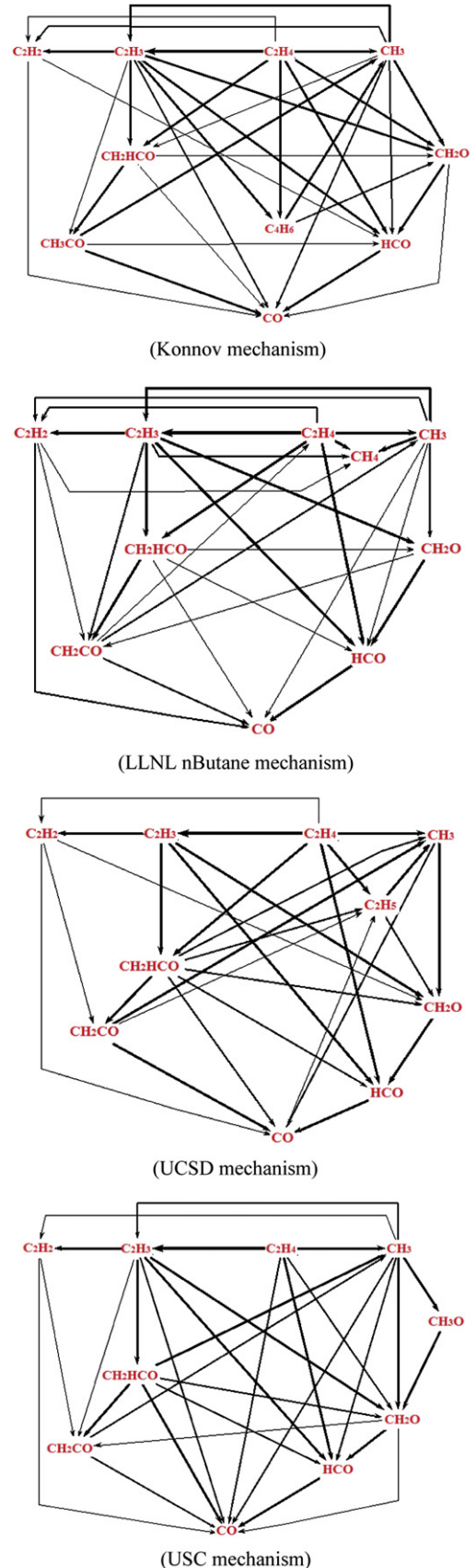


Fig. 7. Pathway analysis in ignition process at the time of $T = 1360$ K for $\theta = 1$, Ar = 92%, $P = 2.1$ atm and initial $T = 1350$ K.

Table 2
Measurements of laminar burning velocities in $C_2H_4/O_2/N_2$ flames.

| Equivalence ratio ϕ | % Diluent $O_2/(N_2 + O_2)$ | P(atm) | T(K) | Experiment method | Ref. |
|--------------------------|-----------------------------|-----------------|--------------------|----------------------------------------------------------------------|------|
| 0.5–1.4 | 18% | 0.5, 1, 2 | 298 | Counter-flow flame/linear extrapolation | [36] |
| | 21% | 1 | | | |
| 0.5–1.4 | 21% | 0.5, 1, 2, 3, 4 | 298 | Outwardly propagating spherical flames/with non-linear extrapolation | [35] |
| 0.5–1.4 | 21% | 1 | 298 | Counter-flow flame/non-linear extrapolation | [33] |
| 0.5–1.4 | 21% | 1, 2, 5 | 298 | Outwardly propagating spherical flames/non-linear extrapolation | [31] |
| 0.6–1.4 | 14%–18% | 1 | 298 | Heat flux method | [32] |
| 0.5–1.4 | 21% | 1 | 298, 360, 400, 470 | counter-flow flame/linear extrapolation | [34] |

OH and subsequent reactions of vinyl with oxygen have important effect on ethylene ignition prediction, however significant variation of the relative importance of various reactions was also observed, which might be attributed to the different reaction routes and rate constants of these reactions in different mechanisms. It is also seen that HCO decomposition reaction and reaction of HCO with O_2 are much more sensitive in the USC and LLNL nButane mechanisms than in the Konnov and UCSD mechanisms.

To better understand the variances among these mechanisms, reaction pathway analysis at the same conditions as the sensitivity analysis was carried out, as shown in Fig. 7. To facilitate the comparison, the time of 10 K initial increase of the temperature ($T = 1360$ K) was selected for the reaction pathway analysis for all mechanisms. The maximum number of species displayed in reaction pathways was limited to 10 according to ranking of the maximum rate of depletion of all species. It can be seen that radicals C_2H_3 and CH_2HCO are consumed in different ways. In the Konnov mechanism, considerable parts of C_2H_3 recombine with C_2H_4 to form C_4H_6 and H, which is important in this mechanism as indicated also by the sensitivity analysis. This reaction is not included in UCSD mechanism and its rate is two orders of magnitude faster than in LLNL nButane mechanism. Moreover, most of CH_2HCO is converted into CO via intermediate production of CH_3CO in the Konnov mechanism, rather than directly decompose to produce CO and CH_3 as in other mechanisms. In USC mechanism, HCO can directly form CO by reaction with C_2H_4 , which is not included in other mechanisms. Besides, reaction $CH_3 + C_2H_4 = C_2H_3 + CH_4$ is not taken into account in UCSD mechanism.

When performing model validation using ignition delays, one should note that the experimental data should be carefully assessed, given the great discrepancies can arise in experimental ignition data due to different ignition criteria and experimental method. Moreover, it is seen that modeling ignition delay times using different criteria have great variations at high temperatures and simulated concentration profiles suggest CH maximum as the ignition criteria from both experimental and model validation consideration. The prediction performance of these models for ignition has been assessed by comparing with experimental data at stoichiometric condition. Some important reactions, such as C_2H_4 initial consumption reactions with radicals O and OH and subsequent reactions of vinyl with oxygen have been identified to exert a significant effect on ethylene ignition prediction. The difference in the reaction rates of these reactions and uncertainties in different mechanisms will be discussed below.

3. Laminar burning velocity

3.1. Available experimental data

Several groups have investigated the laminar burning velocity of premixed ethylene/ O_2/N_2 mixtures at various conditions by using different experimental methods, as summarized in Table 2. These

stretch-corrected laminar burning velocities have been obtained using either counterflow flames or outwardly propagating spherical flames in constant pressure chambers with extrapolation to zero stretch. Experimental data for the laminar burning velocity of C_2H_4 /air mixtures at temperature of 298 K and pressure of 1 atm are shown in Fig. 8. Notable discrepancies are found among existing data, especially for near stoichiometric and rich mixtures, which might be due to different extrapolation methods in dealing with stretch effects on flame speeds. Ji et al. [30] have revealed larger discrepancies toward fuel-rich mixtures between determination of laminar burning velocity using linear and non-linear extrapolations. Jomaas et al. [31] investigated ethylene/air flames at room temperature under both atmospheric and elevated pressures, and pointed out that noticeable differences were observed in the comparison of their experimental data and calculated results. Konnov et al. [32] performed measurements of the adiabatic burning velocity of $C_2H_4/O_2/N_2$ mixtures to determine the effects of composition when oxygen content in synthetic air was varied from 18% to 14% by using the heat flux method which produced non-stretched flames. Hirasawa et al. [33] investigated laminar flames in a counterflow configuration and the laminar burning velocities were obtained through accurate determination of reference speed and stretch by using digital particle image velocimetry (DPIV). Kumar et al. [34] have studied atmospheric pressure laminar flames of premixed $C_2H_4/O_2/N_2$ mixtures in a counterflow configuration with the mixture temperatures varying from 298 to 470 K. Their experimental results were reasonably predicted by two chemical kinetic mechanism (USC and UCSD) at room temperature, while the discrepancy becomes larger with increasing preheat temperature.

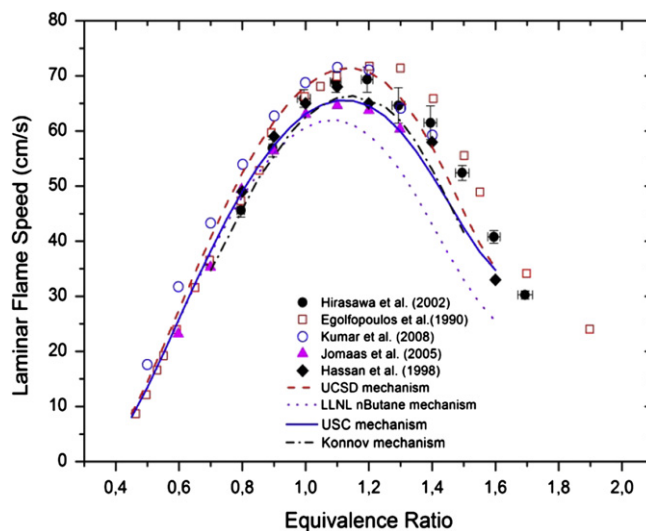


Fig. 8. Comparison of experimental data (symbols) and modeling (lines) of the laminar burning velocities for ethylene/air mixture at temperature 298 K and atmospheric pressure.

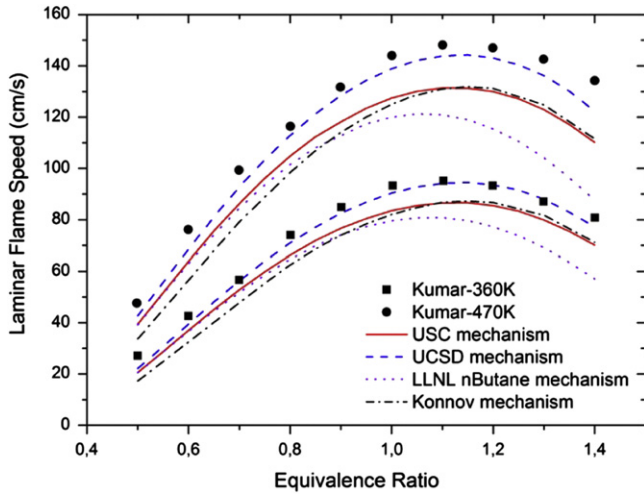


Fig. 9. Comparison of experimental data (symbols) and modeling (lines) for the laminar burning velocities of ethylene/air mixture at atmospheric pressure and temperatures of 360 and 470 K.

3.2. Modeling details

Premixed adiabatic laminar flames have been modeled using Chemkin-Pro [26] under various experimental conditions. Multi-component diffusion and thermal diffusion options were taken into account. Adaptive mesh parameters were $\text{GRAD} = 0.05\text{--}0.1$, and $\text{CURV} = 0.5$. Total number of grid points in these calculations was typically about 160–260, relative and absolute error criteria were $\text{RTOL} = 1\text{E-}4$ and $\text{ATOL} = 1\text{E-}9$.

3.3. Comparison of the experiments and models

The experimental data for $\text{C}_2\text{H}_4/\text{air}$ laminar flames at temperature of 298 K and pressure of 1atm are compared with modeling predictions in Fig. 8. The computed laminar burning velocities using the UCSD mechanism show higher values than other mechanisms, especially for near stoichiometric mixtures, although the modeling well reproduces the experimental data obtained by Kumar et al. [34] using counter-flow flame with linear extrapolation which might be leading to higher results as discussed earlier. The computed results using the Konnov and USC mechanisms are very close and in good agreement with the experimental data obtained by Hassan et al. [35] and Jomaas et al. [31] deduced from outwardly propagating spherical flames with non-linear extrapolation method. The small variance in the prediction using the Konnov mechanism shows lower laminar burning velocity for lean mixtures than USC mechanism. The modeling using LLNL nButane mechanism shows indistinguishable results with the modeling using USC mechanism for the mixtures with equivalence ratios less than 0.9, however significant underprediction by LLNL nButane model has been found for near stoichiometric and rich mixtures.

Since most of practical applications are not at room temperature and atmospheric pressure, it is important to assess modeling predictions for the laminar burning velocity of $\text{C}_2\text{H}_4/\text{air}$ mixtures at these elevated conditions. Comparisons between experimental and modeling results at preheat unburned mixture temperature and elevated pressures have been conducted, as respectively shown in Figs. 9 and 10. As shown in Fig. 9, the models' behaviors for $\text{C}_2\text{H}_4 + \text{N}_2(79\%) + \text{O}_2(21\%)$ mixture at temperatures of 360 K and 470 K are similar to that at 298 K, the discrepancies of modeling prediction increase with the preheat temperature increasing. It was

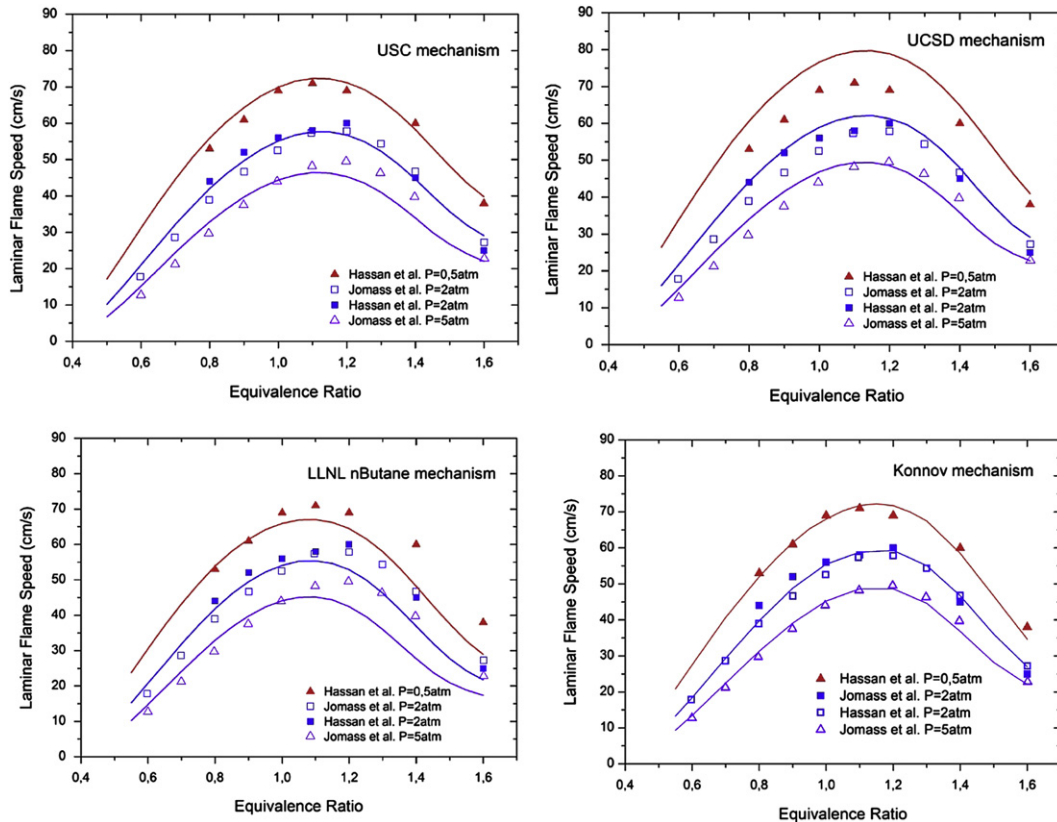


Fig. 10. Comparison of experimental data (symbols) and modeling (lines) for the laminar burning velocities of ethylene/air mixture at room temperature and pressures of 0.5, 2, and 5 atm.

found that the difference of the modeling results between the Konnov mechanism and USC mechanism for the preheat temperature of 470 K is about 6 cm/s at equivalent ratio of 0.5, and the difference of the modeling results at the preheat temperature of 470 K between LLNL nButane mechanism and USC mechanism is as much as about 22 cm/s at equivalent ratio of 1.4.

Fig. 10 presents comparison of experimental data at different pressures obtained by Hassan et al. [35] and Jomaas et al. [31] and modeling results. The modeling results using USC mechanism indicates good prediction at the pressure of 0.5 atm and 2 atm, and slight underprediction of the laminar burning velocities for rich mixtures at the pressure of 5 atm. The modeling results using UCSD mechanism show a satisfactory prediction at the pressures of 2 atm and 5 atm, however, significant overprediction have been found at the pressure of 0.5 atm for mixtures with equivalent ratios less than 1.4. As observed earlier, the modeling results of LLNL nButane mechanism indicate a good agreement with available experimental data for lean mixtures, however, underprediction for rich mixtures becomes severe as the pressure increasing. The modeling results of the Konnov mechanism have shown the best agreement with the experimental data at all equivalence ratios and pressures studied.

Recently Konnov et al. [32] have investigated the effect of variation of the oxidizer composition on the burning velocity of ethylene/ N_2/O_2 mixture using the heat flux method. The mole fraction of oxygen in the $N_2 + O_2$ mixture was defined by dilution factor D ($D = O_2/(O_2 + N_2)$), and varied from 18% to 14%. Fig. 11 shows comparison of these experimental data and modeling results. The experimental adiabatic burning velocities of $D = 0.18$ mixture obtained by Konnov et al. [32] shows good consistency with the experimental data obtained by Egolfopoulos et al. [36] in lean flames, while, as discussed earlier, Egolfopoulos et al. obtained higher values in rich flames using linear extrapolation of stretch in

counterflow flames. It can be seen that models presented in Fig. 11 show generally good predictions of the laminar burning velocity at these conditions, however, some discrepancies still exist. The USC model shows satisfactory agreement with the presented experimental data. The UCSD model overpredicts the experimental data at near stoichiometric region for $D = 0.18$ condition. The LLNL nButane model shows notably lower values than the measurement in rich region for all conditions. The Konnov model seems under-predict the experimental results over entire range of equivalent ratios, especially for $D = 0.14$.

3.4. Modeling analysis

To further understand the models' behavior and identify important reactions, sensitivity analysis for laminar burning velocity of ethylene/air mixtures at fuel-lean ($\Phi = 0.7$), stoichiometric and fuel-rich ($\Phi = 1.4$) conditions has been performed, as shown in Fig. 12. The reactions manifested in the sensitivity analysis are listed in Table 3. It is seen that H–O and C_1 chemistry reactions significantly influence the laminar burning velocity in lean ethylene/air flames, and C_2 chemistry reactions become comparably sensitive to C_1 chemistry in fuel-rich flames. Reaction R1: $H + O_2 = O + OH$, as the main branching process, has crucial effect on the laminar burning velocity for all equivalence ratios studied, and the normalized sensitivity coefficient of this reaction increases when the mixture varies from lean to rich conditions. CO oxidation reaction R8: $CO + OH = CO_2 + H$, as the most important heat release and H-producing step, is dominant for fuel-lean flames and important in the stoichiometric flame. Reactions converting HCO to CO are considerably sensitive for the prediction of the laminar burning velocities at both lean and rich flame conditions. For all mechanisms, H-producing decomposition reaction R9:

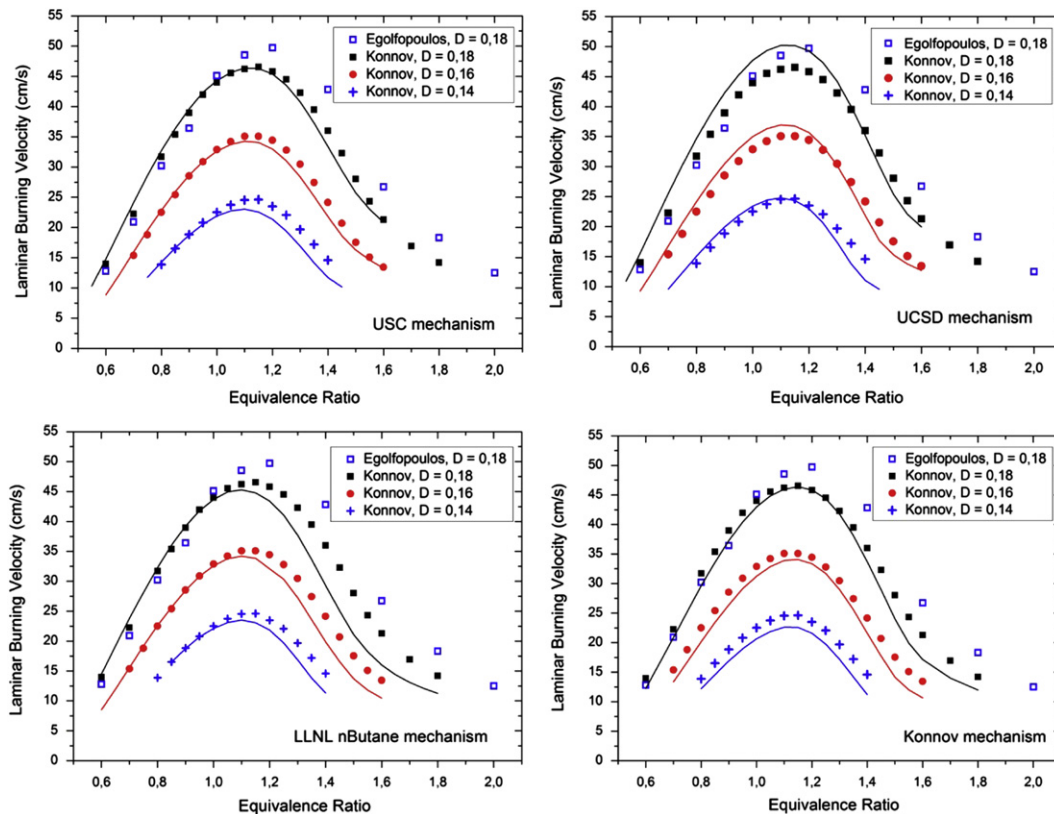


Fig. 11. Comparison of experimental data (symbols) and modeling (lines) for the laminar burning velocities for ethylene/ O_2/N_2 mixture with oxygen content varying within $D = 0.18$ – 0.14 at 298 K, $P = 1$ atm.

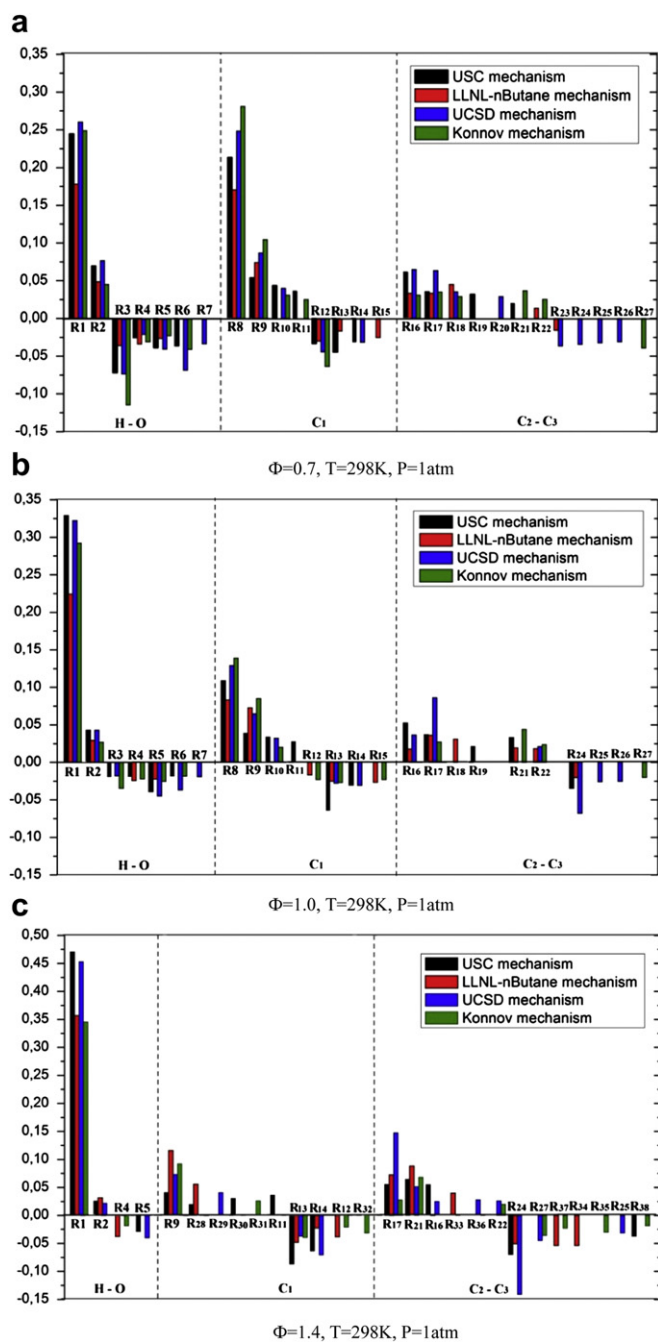


Fig. 12. Normalized sensitivity coefficients for the laminar burning velocity of ethylene/air mixture at $T = 298\text{ K}$, $P = 1\text{ atm}$ (Top: lean $\Phi = 0.7$; middle: stoichiometric; bottom: rich $\Phi = 1.4$).

$\text{HCO} + \text{M} = \text{CO} + \text{H} + \text{M}$ competes with reaction R12: $\text{HCO} + \text{O}_2 = \text{CO} + \text{HO}_2$ in fuel-lean flames and terminating reaction R13: $\text{HCO} + \text{H} = \text{CO} + \text{H}_2$ in fuel-rich flames. In the USC mechanism, reaction R13 exhibits higher sensitivity coefficients for all mixtures, and reaction R9 is less sensitive for stoichiometric and fuel-rich flames, which is different from other mechanisms. From C_2 chemistry, reactions of C_2H_4 with radicals O and OH show a notable sensitivity for lean flame conditions, while have little effect only in USC and UCSD mechanisms for fuel-rich flames. Reaction R17: $\text{C}_2\text{H}_3 + \text{O}_2 = \text{CH}_2\text{HCO} + \text{O}$, acting as a chain-branching reaction, have a positive sensitivity coefficients for all equivalence ratios studied. Decomposition reaction R21: $\text{C}_2\text{H}_3(+\text{M}) = \text{C}_2\text{H}_2 + \text{H}(+\text{M})$

shows a positive sensitivity in fuel-rich flames for all mechanisms, while reaction R24: $\text{C}_2\text{H}_3 + \text{H} = \text{C}_2\text{H}_2 + \text{H}_2$ shows an inhibition effect as a terminating reaction in fuel-rich flames for the USC, LLNL-nButane and UCSD mechanisms. It is also found that reactions (R17) and (R24) show much higher sensitivity in UCSD mechanism than in other mechanisms, while reaction R21 in the Konnov mechanism has more important effect comparing with reactions (R17) and (R24) at fuel rich conditions. Also notable that reactions involving higher hydrocarbons through recombination reactions at fuel-rich conditions do not show important influence on the laminar burning velocity prediction.

4. Reaction analysis

According to the sensitivity analyses of ignition and flame propagation, reactions involving C_2H_4 and vinyl chemistry show considerable importance in ethylene oxidation process. The kinetic data for these reactions needs to be carefully considered for further improving predicting performance of ethylene combustion models, especially for fuel rich conditions. The differences in the reaction rate constants and routes among four mechanisms are presented and discussed as following.

$\text{C}_2\text{H}_4 + \text{OH}$: For reactions $\text{C}_2\text{H}_4 + \text{OH}$, only the Konnov mechanism takes additional reaction products $\text{CH}_2\text{O} + \text{CH}_3$ into account as an important pathway for low and moderate temperature chemistry, which converts active radical OH into relatively inactive radical CH_3 .

$\text{C}_2\text{H}_4 + \text{O}$: For reactions $\text{C}_2\text{H}_4 + \text{O}$, production channel $\text{CH}_2\text{HCO} + \text{H}$ is not included in USC mechanism, however, as shown in Fig. 6, it is considerably important in UCSD and LLNL nButane mechanisms. Only USC and the Konnov mechanisms consider H abstraction route to produce $\text{C}_2\text{H}_3 + \text{OH}$ which is important reaction channel and contributes more than one third in C_2H_4 consumption by reaction with O in both mechanisms.

$\text{C}_2\text{H}_3 + \text{O}_2$: Reaction between vinyl and molecular oxygen very significantly influences both ignition and flame propagation. For reactions $\text{C}_2\text{H}_3 + \text{O}_2$, reaction channel $\text{CH}_2\text{HCO} + \text{O}$ is considered as main reaction channel, and as a chain branching reaction, it can be very important and sensitive for ethylene ignition and flames. It is found that this reaction rate in USC mechanism is four times higher than in the Konnov and LLNL nButane mechanism, and twice higher than in UCSD mechanism. In addition, $\text{C}_2\text{H}_2 + \text{HO}_2$ is much more important channel for reactions $\text{C}_2\text{H}_3 + \text{O}_2$ in the Konnov and LLNL nButane mechanisms compared to USC and UCSD mechanisms. The reaction rates analysis also revealed that C_2H_3 consumption in USC mechanism is faster than in other mechanisms.

$\text{C}_2\text{H}_3(+\text{M}) = \text{C}_2\text{H}_2 + \text{H}(+\text{M})$: This reaction has been identified as a relatively important in fuel-rich flames for all four mechanisms, while significant differences in rate constants have been found. The rate constant in the Konnov mechanism is about twice and five times higher than in the USC and UCSD mechanisms respectively at 1800 K, while it becomes about five and twenty times higher than in the USC and UCSD mechanisms respectively at temperature of 1000 K.

$\text{C}_2\text{H}_3 + \text{H} = \text{C}_2\text{H}_2 + \text{H}_2$: this reaction has also been found as an important inhibition step in fuel-rich flames in the USC, UCSD and LLNL-nButane mechanism. The reaction rate constant in USC mechanism is more than twice higher than in the UCSD and LLNL-nButane mechanism, and more than seven times higher than in the Konnov mechanism.

One should note that complicated picture of the sensitivity spectra shown in Fig. 12 is largely defined by the choice of rate constants and by inclusion/omission of some channels considered to be minor as summarized in Table 3. Therefore, direct variation of the rate constants of most sensitive reactions could be misleading if the list of reactions is incomplete, or may lead to deterioration of predictive performance of a given model for other fuels included.

Table 3
Reactions manifested in flame sensitivity analysis.

| No. | Reaction | $\Phi = 0.7$ | | | | $\Phi = 1.0$ | | | | $\Phi = 1.4$ | | | |
|--------------------------------|--------------------------------------------------------------------------------------------------|-------------------------------------------------------------------------------------------|------------------|------------------|----------------------------|--------------|------------------|------------------|----------------------------|--------------|------------------|------------------|----------------------------|
| | | U S C | U C S D | L L N L | K o n n o v | U S C | U C S D | L L N L | K o n n o v | U S C | U C S D | L L N L | K o n n o v |
| H–O | R1 ^a | H + O ₂ = O + OH | * | * | * | * | * | * | * | * | * | * | * |
| | R2 | HO ₂ + H = OH + OH | + | + | + | + | + | + | + | + | + | + | – |
| | R3 | H + O ₂ (+M) = HO ₂ (+M) | + | + | + | * | + | + | – | + | – | – | – |
| | R4 ^b | HO ₂ + H = H ₂ + O ₂ | + | + | + | + | + | – | + | + | – | – | + |
| | R5 | H + OH + M = H ₂ O + M | + | + | + | + | + | + | + | + | + | – | – |
| | R6 | OH + HO ₂ = H ₂ O + O ₂ | + | + | – | + | + | + | – | + | – | – | – |
| | R7 | OH + O + M = HO ₂ + M | – | + | – | – | – | + | – | – | – | – | – |
| C ₁ | R8 | CO + OH = CO ₂ + H | * | * | * | * | * | + | * | – | – | – | – |
| | R9 | HCO + M = CO + H + M | + | + | + | * | + | + | + | + | + | * | + |
| | R10 | CH ₃ + OH = CH ₂ (s) + H ₂ O | + | + | – | + | + | + | – | + | – | – | – |
| | R11 | CH ₃ + HO ₂ = CH ₃ O + OH | + | – | – | + | + | – | – | – | – | – | – |
| | R12 | HCO + O ₂ = CO + HO ₂ | + | + | + | + | – | – | + | + | – | – | + |
| | R13 | HCO + H = CO + H ₂ | + | – | + | – | + | + | + | + | + | + | + |
| | R14 | CH ₃ + H(+M) = CH ₄ (+M) | + | + | – | – | + | + | – | – | + | + | – |
| | R15 | HCO + OH = H ₂ O + CO | – | – | + | – | – | – | + | + | – | – | – |
| | R28 | CH ₂ (s) + O ₂ = H + OH + CO | – | – | – | – | – | – | – | – | + | – | + |
| | R29 | CH ₂ + O ₂ = H + OH + CO | ○ | – | – | – | ○ | – | – | – | ○ | + | – |
| | R30 | CH ₂ + O ₂ = HCO + OH | – | ○ | – | – | – | ○ | – | – | ○ | – | – |
| | R31 | CH ₂ + O ₂ = CH ₂ O + O | ○ | ○ | – | – | ○ | ○ | – | – | ○ | – | + |
| | R32 | CH ₂ (s) + H ₂ O => CH ₃ OH | – | ○ | ○ | – | – | ○ | ○ | – | – | ○ | ○ |
| C ₂ –C ₃ | R16 | C ₂ H ₄ + OH = C ₂ H ₃ + H ₂ O | + | + | + | + | + | + | + | – | + | + | – |
| | R17 | C ₂ H ₃ + O ₂ = CH ₂ CHO + O | + | + | + | + | + | + | + | + | + | * | + |
| | R18 | C ₂ H ₄ + O = CH ₂ CHO + H | ○ | + | + | + | ○ | – | – | – | ○ | – | – |
| | R19 | C ₂ H ₄ + O = C ₂ H ₃ + OH | + | ○ | ○ | – | + | ○ | ○ | – | – | ○ | ○ |
| | R20 | CH ₂ CO + O = CH ₂ + CO ₂ | – | + | – | ○ | – | – | – | ○ | – | – | – |
| | R21 ^c | C ₂ H ₃ (+M) = C ₂ H ₂ + H(+M) | + | – | – | + | + | – | + | + | + | + | + |
| | R22 | C ₂ H ₂ + O = HCCO + H | – | – | + | – | – | + | + | + | + | + | + |
| | R23 | C ₂ H ₄ + O = CH ₃ + HCO | – | + | + | – | – | – | – | – | – | – | – |
| | R24 | C ₂ H ₃ + H = C ₂ H ₂ + H ₂ | – | + | – | – | – | + | + | – | + | * | + |
| | R25 | CH ₂ CO + H = CH ₃ + CO | – | + | – | – | – | + | – | – | – | + | – |
| | R26 | C ₂ H ₅ (+M) = C ₂ H ₄ + H(+M) | – | + | – | – | – | + | – | – | – | – | – |
| | R27 ^d | C ₂ H ₃ + CH ₃ (+M) = C ₃ H ₆ (+M) | ○ | – | – | + | – | – | – | + | – | – | – |
| | R33 | HCCO + O ₂ = HCO + CO + O | ○ | ○ | – | ○ | ○ | ○ | – | ○ | ○ | ○ | + |
| | R34 | HCCO + H = CH ₂ (s) + CO | – | – | – | ○ | – | – | – | ○ | – | – | + |
| | R35 | HCCO + H = CH ₂ + CO | ○ | ○ | ○ | – | ○ | ○ | ○ | – | ○ | ○ | ○ |
| | R36 | C ₂ H ₄ + H = C ₂ H ₃ + H ₂ | – | – | – | – | – | – | – | – | – | + | – |
| R37 | C ₂ H ₃ + O ₂ = C ₂ H ₂ + HO ₂ | – | – | – | – | – | – | – | – | – | – | + | |
| R38 | CH ₃ + CH ₃ = C ₂ H ₆ + H | – | – | – | – | – | – | – | – | + | – | – | |

*: |sensitivity coefficient| > 0.1; +: sensitive; –: non-sensitive; ○: absent.

^a The reverse reaction is used in LLNL-nButane mechanism.

^b The reverse reaction is used in USC mechanism.

^c The reverse reaction is used in LLNL-nButane mechanism.

^d C₃H₆ = C₂H₃ + CH₃ is used in Konnov and LLNL-nButane mechanism.

5. Conclusions

Development of a single detailed kinetic mechanism suitable for the modeling of combustion of different fuels including alkanes, alkenes, oxygenated species, etc. is a challenging task. In the present work, several contemporary comprehensive detailed kinetic mechanisms for ethylene combustion, including the Konnov mechanism, LLNL nButane mechanism, San Diego mechanism and USC mechanism have been extensively validated by comparing with available experimental data for ethylene ignition and flame propagation under a variety of conditions. The discrepancies of these models' behavior have been observed and further sensitivity analysis for each mechanism has been performed to identify important reactions for the prediction of ethylene ignition and flames. Reactions involving initial consumption reactions with radicals O and OH and subsequent reactions of vinyl with oxygen have significant effect on ethylene ignition. In addition, the sensitivity analysis of the flame

propagation indicate that H–O and C₁ chemistry reactions significantly influence the laminar burning velocity in lean ethylene/air flames, while C₂ chemistry reactions become increasingly sensitive in fuel-rich flames. Furthermore, reaction-by-reaction analysis has been conducted to look inside the models. Remarkable variation of the reaction routes and rate constants of reactions involving C₂H₄ and vinyl chemistry have been found in different mechanisms, which has been considered to lead to the different modeling behaviors. Due to still remaining uncertainties, reactions involving C₂H₄ and vinyl chemistry need to be accurately re-evaluated for further development of detailed chemical mechanisms for ethylene combustion.

Acknowledgment

China Scholarship Council is gratefully acknowledged for the grant to C. Xu.

References

- [1] Ren T, Patel MK, Blok K. Steam cracking and methane to olefins: energy use, CO₂ emissions and production costs. *Energy* 2008;33:817–33.
- [2] Colket MB, Spadaccini LJ. Scramjet fuels autoignition study. *J Propuls Power* 2001;17(2):315–23.
- [3] Konnov AA. Implementation of the NCN pathway of prompt-NO formation in the detailed reaction mechanism. *Combust Flame* 2009;156(11):2093–105.
- [4] LLNL mechanism available at: https://www-pls.llnl.gov/?url=science_and_technology-chemistry-combustion-ch4.
- [5] Chemical Kinetic Mechanism for Combustion Application. Center for Energy research, University of California at San Diego.
- [6] Wang Hai, You Xiaoping, Joshi Ameya V, Davis Scott G, Laskin Alexander, Egolfopoulos Fokion, et al. USC mech version II. High-temperature combustion reaction model of H₂/CO/C₁–C₄ compounds, http://ignis.usc.edu/USC_Mech_II.htm; May 2007.
- [7] Marinov NM, Pitz WJ, Westbrook CK, Vincitore AM, Castaldi MJ, Senkan SM. Aromatic and polycyclic aromatic hydrocarbon formation in a laminar premixed n-butane flame. *Combust Flame* 1998;114:192–213.
- [8] Schultz E, Shepherd J. Validation of detailed reaction mechanisms for detonation simulation. Pasadena, CA: Explosion Dynamic Lab GALCIT, California Institute of Technology; 2000. Rept FM99–5.
- [9] Varatharajan B, Williams FA. Ethylene ignition and detonation chemistry, part 1: detailed modeling and experimental comparison. *J Propulsion Power* 2002;18(2):344–51.
- [10] Gay ID, Glass GP, Kern RD, Kistiakowsky GB. Ethylene–Oxygen reaction in shock waves. *J Chem Phys* 1967;47(1):313–20.
- [11] Homer JB, Kistiakowsky GB. Oxidation and pyrolysis of ethylene in shock waves. *J Chem Phys* 1967;47(12):5290–5.
- [12] Drummond LJ. Shock-initiated exothermic reactions.V. Oxidation of ethylene. *Aust J Chem* 1968;21(11):2641–8.
- [13] Baker JA, Skinner GB. Shock-tube studies on the ignition of ethylene-oxygen-argon mixtures. *Combust Flame* 1972;19(3):347–50.
- [14] Suzuki M, Moriwaki T, Okazaki S, Okuda T, Tanzawa T. Oxidation of ethylene in shock-tube. *Astronautica Acta* 1973;18(5):359–65.
- [15] Jachimowski CJ. An experimental and analytical study of acetylene and ethylene oxidation behind shock waves. *Combust Flame* 1977;29:55–66.
- [16] Hidaka Y, Kataoka T, Suga M. Shock-tube investigation of ignition in ethylene-oxygen-argon mixtures. *B Chem Soc Jpn* 1974;47(9):2166–70.
- [17] Hidaka Y, Nishimori T, Sato K, Henmi Y, Okuda R, Inami K, et al. Shock-tube and modeling study of ethylene pyrolysis and oxidation. *Combust Flame* 1999;117(4):755–76.
- [18] Brown CJ, Thomas GO. Experimental studies of shock-induced ignition and transition to detonation in ethylene and propane mixtures. *Combust Flame* 1999;117(4):861–70.
- [19] Cadman P, Bambrey RJ, Box SK, Thomas GO. Ethylene combustion studied over a wide temperature range in high-temperature shock waves. *Combust Sci Technol* 2002;174(11–12):111–27.
- [20] Horning DC. A study of the high-temperature autoignition and thermal decomposition of hydrocarbons. Report No TSD-135; 2001.
- [21] Kalitan DM, Hall JM, Petersen EL. Ignition and oxidation of ethylene-oxygen-diluent mixtures with and without silane. *J Propulsion Power* 2005;21(6):1045–56.
- [22] Penyazkov OG, Sevrouk KL, Tangirala V, Joshi N. High-pressure ethylene oxidation behind reflected shock waves. *P Combust Inst* 2009;32(2):2421–8.
- [23] Saxena S, Kahandawala MSP, Sidhu SS. A shock tube study of ignition delay in the combustion of ethylene. *Combust Flame* 2011;158(6):1019–31.
- [24] Hanson RK. Applications of quantitative laser sensors to kinetics, propulsion and practical energy systems. *P Combust Inst* 2011;33(1):1–40.
- [25] Hai Wang, Alexander Laskin. A Comprehensive Kinetic model of ethylene and acetylene oxidation at high temperatures, USC, available at: <http://ignis.usc.edu/Mechanisms/C2-C4/c2.pdf>.
- [26] Chemkin-Pro. Reaction Design Inc., <http://www.reactiondesign.com/>.
- [27] Wangher A, Quinard J, Searby G. Experimental and numerical investigations of the relation between OH* emission, flame speed and mass consumption rate. In: Proc. of the 3rd European Combustion Meeting, Chania, Crete, Greece; 2007.
- [28] Hall JM, Rickard MJA, Petersen EL. Comparison of characteristic time diagnostics for ignition and oxidation of fuel/oxidizer mixtures behind reflected shock waves. *Combust Sci Technol* 2005;177:455–83.
- [29] Haber LC, Vandsburger U. A global reaction model for OH* chemiluminescence applied to a laminar flat-flame burner. *Combust Sci Technol* 2003;175:1859–91.
- [30] Ji C, Dames E, Wang YL, Wang H, Egolfopoulos FN. Propagation and extinction of premixed C₅–C₁₂ n-alkane flames. *Combust Flame* 2010;157(2):277–87.
- [31] Jomaas G, Zheng XL, Zhu DL, Law CK. Experimental determination of counterflow ignition temperatures and laminar flame speeds of C₂–C₃ hydrocarbons at atmospheric and elevated pressures. *P Combust Inst* 2005;30(1):193–200.
- [32] Konnov AA, Dyakov IV, De Ruyck J. The effects of composition on the burning velocity and NO formation in premixed flames of C₂H₄ + O₂ + N₂. *Exp Thermal Fluid Sci* 2008;32(7):1412–20.
- [33] Hirasawa T, Sung CJ, Joshi A, Yang Z, Wang H, Law CK. Determination of laminar flame speeds using digital particle image velocimetry: binary fuel blends of ethylene, n-Butane, and toluene. *P Combust Inst* 2002;29(2):1427–34.
- [34] Kumar K, Mittal G, Sung C-J, Law CK. An experimental investigation of ethylene/O₂/diluent mixtures: laminar flame speeds with preheat and ignition delays at high pressures. *Combust Flame* 2008;153(3):343–54.
- [35] Hassan MI, Aung KT, Kwon OC, Faeth GM. Properties of laminar premixed hydrocarbon/air flames at various pressures. *J Propulsion Power* 1998;14(4):479–88.
- [36] Egolfopoulos FN, Zhu DL, Law CK. Experimental and numerical determination of laminar flame speeds: mixtures of C₂-hydrocarbons with oxygen and nitrogen. *Symposium (International) Combust* 1991;23(1):471–8.